A&A 451, 259–266 (2006)
DOI: 10.1051/0004-6361:20054155

Astronomy & Astrophysics

Spectral energy distribution of the γ-ray microquasar LS 5039

J. M. Paredes[1], V. Bosch-Ramon[1], and G. E. Romero[2,3,⋆]

[1] Departament d'Astronomia i Meteorologia, Universitat de Barcelona, Av. Diagonal 647, 08028 Barcelona, Spain
e-mail: jmparedes@ub.edu;vbosch@am.ub.es
[2] Instituto Argentino de Radioastronomía, C.C.5, (1894) Villa Elisa, Buenos Aires, Argentina
e-mail: romero@iar.unlp.edu.ar
[3] Facultad de Ciencias Astronómicas y Geofísicas, UNLP, Paseo del Bosque, 1900 La Plata, Argentina
e-mail: romero@fcaglp.unlp.edu.ar

Received 5 September 2005 / Accepted 24 January 2006

ABSTRACT

The microquasar LS 5039 has recently been detected as a source of very high energy (VHE) γ-rays. This detection, that confirms the previously proposed association of LS 5039 with the EGRET source 3EG J1824−1514, makes of LS 5039 a special system with observational data covering nearly all the electromagnetic spectrum. In order to reproduce the observed spectrum of LS 5039, from radio to VHE γ-rays, we have applied a cold matter dominated jet model that takes into account accretion variability, the jet magnetic field, particle acceleration, adiabatic and radiative losses, microscopic energy conservation in the jet, and pair creation and absorption due to the external photon fields, as well as the emission from the first generation of secondaries. The radiative processes taken into account are synchrotron, relativistic Bremsstrahlung and inverse Compton (IC). The model is based on a scenario that has been characterized with recent observational results, concerning the orbital parameters, the orbital variability at X-rays and the nature of the compact object. The computed spectral energy distribution (SED) shows a good agreement with the available observational data.

Key words. X-rays: binaries – stars: winds, outflows – gamma rays: observations – stars: individual: LS 5039 – gamma rays: theory

1. Introduction

Microquasars are radio emitting X-ray binaries with relativistic radio jets (Mirabel & Rodríguez 1999). LS 5039 was classified as microquasar when non-thermal radiation produced in a jet was detected with the VLBA (Paredes et al. 2000). New observations conducted later with the EVN and MERLIN confirmed the presence of an asymmetric two-sided persistent jet reaching up to ∼1000 AU on the longest jet arm (Paredes et al. 2002; Ribó 2002). LS 5039 is a high mass X-ray binary (Motch et al. 1997) whose optical counterpart is a bright ($V \sim 11$) star of spectral type O6.5V((f)) (Clark et al. 2001). Although McSwain et al. (2001, 2004) first derived the period and the orbital parameters of the system, new values of the orbital period ($P_{\rm orb} = 3.9060 \pm 0.0002$ days, with periastron passage associated to $T_0 = \mathrm{HJD}\ 2\,451\,943.09 \pm 0.10$), eccentricity ($e = 0.35 \pm 0.04$), phase of periastron passage (0.0), and inclination (assuming pseudo-synchronization, $i = 24.9 \pm 2.8°$) have been reported by Casares et al. (2005), who place the system at a distance of 2.5 ± 0.1 kpc. The radius of the companion star is moderately close to the Lagrange point during periastron but without overflowing the Roche lobe. In addition, Casares et al. (2005) state that the compact object in LS 5039 is a black hole of mass $M_{\rm X} = 3.7^{+1.3}_{-1.0}\ M_\odot$. At X-rays, the spectrum of the source follows a power-law and the fluxes are moderate and variable, with temporal scales similar to the orbital period. The variability is likely associated with changes in the accretion rate due to the motion of the compact object along an eccentric orbit (Bosch-Ramon et al. 2005a).

Among microquasars, LS 5039 is specially relevant for its proposed association with 3EG J1824−1514 (Paredes et al. 2000), an unidentified source in the 3rd EGRET catalog of high-energy γ-ray sources (>100 MeV; Hartman et al. 1999). Recently, Aharonian et al. (2005a), using the High Energy Stereoscopic System (HESS), have detected LS 5039 at energies above 250 GeV. This detection, that confirms the high-energy γ-ray nature of LS 5039 (Paredes et al. 2000), gives strong support to the idea that microquasars are a distinctive class of high- and very high-energy γ-ray sources. The confirmation of LS 5039 as a high-energy γ-ray source, combined with the fact of being a runaway microquasar ejected from the Galactic plane at ∼150 km s^{-1} (Ribó et al. 2002), strongly raises the question about the connection between some of the remaining unidentified, faint, variable, and soft γ-ray EGRET sources and possible microquasar systems above/below the Galactic plane (e.g., Kaufman Bernadó et al. 2002; Romero et al. 2004; Bosch-Ramon et al. 2005b).

⋆ Member of CONICET.

LS 5039 was also proposed to be the counterpart of a COMPTEL source (∼1 MeV) (Strong et al. 2001) and BATSE detected it at soft γ-rays (Harmon et al. 2004). In addition to LS 5039, there is another microquasar, LS I +61 303 (Massi et al. 2004), that is likely associated with an EGRET source (Kniffen et al. 1997). Both microquasars have been extensively studied at different wavelengths, and both have a very similar spectral energy distribution. Bosch-Ramon & Paredes (2004a,b) have explored with a detailed numerical leptonic model whether these systems can produce the level of emission detected by EGRET (>100 MeV), and the observed variability. At VHE, Aharonian et al. (2005b) argue in favor of hadronic origin of TeV photons in case that γ-rays are produced within $\sim 10^{12}$ cm, and Dermer & Böttcher (2006) point to combined star IC and synchrotron self-Compton (SSC) emission to explain the different epoch detections by EGRET and HESS, respectively.

To explain both, the observed spectrum of LS 5039 from radio to VHE γ-rays and the variability, we have applied a broad-band emission model, based on a freely expanding magnetized jet dynamically dominated by cold protons and radiatively dominated by relativistic leptons (Bosch-Ramon et al. 2006). In this paper we present the results obtained after applying such model to LS 5039. The compiled observational data covering the full electromagnetic spectrum is given in Sect. 2. In Sect. 3 a brief description of the model is provided, and the parameters of the model are discussed. The results obtained for LS 5039 are presented in Sect. 4, and the work is summarized in Sect. 5.

2. Observational data of LS 5039

We compile here the observational data from the literature. The radio data, obtained at 20, 6, 3.5 and 2 cm wavelengths with the VLA, are from Martí et al. (1998). The optical and infrared data, covering the bands *UBVRIJHKL*, are from Clark et al. (2001) and Drilling (1991), and have been corrected for absorption ($A_V = 4.07$, Casares et al. 2005). The X-ray data (3–30 keV), obtained with RXTE, are from Bosch-Ramon et al. (2005a), being diffuse background subtracted. The (20–430 keV) data, obtained with the BATSE Earth occultation technique, are from Harmon et al. (2004). The (1–30 MeV) data are from Zhang et al. (2005), obtained with COMPTEL, whose flux values, however, should be taken as an upper limit. This is due to the source region defined by the COMPTEL γ-ray source, GRO J1823−12, at galactic coordinates ($l = 17.5°$, $b = -0.5°$), contains in addition to LS 5039/3EG J1824−1514 two additional EGRET sources (Collmar et al. 2003, Zhang et al. 2005). The high-energy γ-ray data have been taken from the third EGRET catalog of high-energy γ-ray sources (>100 MeV; Hartman et al. 1999). The VHE γ-ray (>100 GeV) data, obtained with HESS, are from Aharonian et al. (2005a). The values of the magnitudes and fluxes have been transformed in luminosities using the updated value for the distance of 2.5 kpc (Casares et al. 2005). All these observational data are plotted in Fig. 3.

2.1. X-ray lightcurve

The X-ray lightcurve of LS 5039 observed by RXTE, folded in phase with the new orbital period value, shows a clear smooth peak at phase 0.8 and another marginal one at phase 0.3 (Bosch-Ramon et al. 2005a). This lightcurve is hardly explained by accretion through a spherically symmetric wind of a typical O type star, due to the high velocities of the wind at infinity, and also because of the constraints on the stellar mass loss rate ($\lesssim 10^{-6}\ M_\odot\ \mathrm{yr}^{-1}$, Casares et al. 2005). It has been proposed that certain asymmetries in the wind could produce these peaks in the X-ray lightcurve (Bosch-Ramon et al. 2005a).

3. Modeling

3.1. An accretion model for LS 5039

To reproduce approximately the variations in the X-rays, we have assumed the existence of a relatively slow equatorial wind (outflowing velocity $\sim 6 \times 10^7$ cm s^{-1}) that would increase the accretion rate up to the (moderate) levels required by the observed emission in the context of our model, and would produce a peak after periastron. Although the existence of low velocity flows is not yet well established, it seems that it would not be a rare phenomenon among the massive wind accreting X-ray binaries. This is, for instance, the case of the O9.5V star BD +53°2790, whose ultraviolet spectrum reveals an abnormally slow wind velocity for its spectral type (Ribó et al. 2006). Only a small fraction of the wind being slower at the equator is enough to increase significantly the accretion rate along the orbit if one assumes pseudo-synchronization. In this case, the orbital plane and the plane perpendicular to companion star rotation axis will be likely the same (Casares et al. 2005), allowing for the compact object to accrete from this slow equatorial wind all along the orbit.

To explain the second peak we have introduced a stream, with a velocity of 5×10^6 cm s^{-1} and an additional mass loss rate of ∼1% of the normal wind, that is formed near periastron passage when the attraction force between the two components of the system is at its maximum. This slower matter stream would produce a very delayed peak at phase 0.7. The formation of a matter stream, due to gravitational stress at the smallest orbital distances, is not unusual in close binary systems like LS 5039. We have used the approach followed by Leahy (2002) to explain the X-ray lightcurve of GX 302–1, also with a peak before periastron passage. Although there is still a shift of 0.1 in phase between the model peaks and the observed ones, it is important to note that there is likely an accretion disk, and the matter that reaches the disk spends some time in it until part of this matter is ejected as a jet (a lower-limit for the accretion time is the free fall time, implying a shift of ∼0.06 in phase, when falling from 10^{12} cm). The accretion rate evolution obtained from the model described here is shown in Fig. 1.

3.2. A leptonic jet model for LS 5039 broad-band emission

A new model based on a freely expanding magnetized jet, whose internal energy is dominated by a cold proton plasma

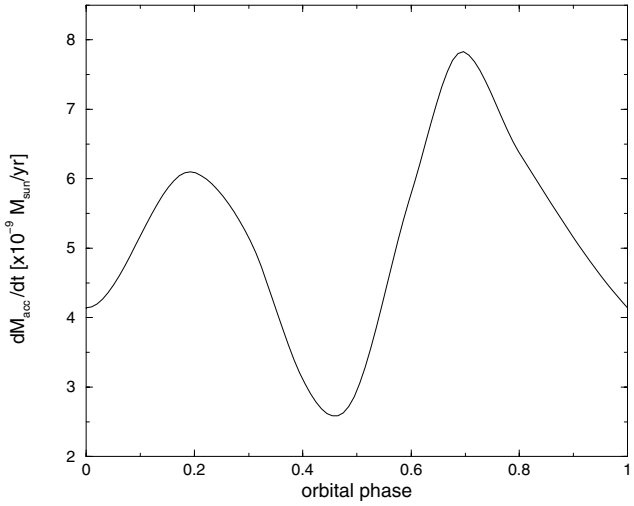

Fig. 1. Accretion curve along an orbital period inferred from the observed X-ray lightcurve in Bosch-Ramon et al. (2005a), adopting the accretion model developed for this work.

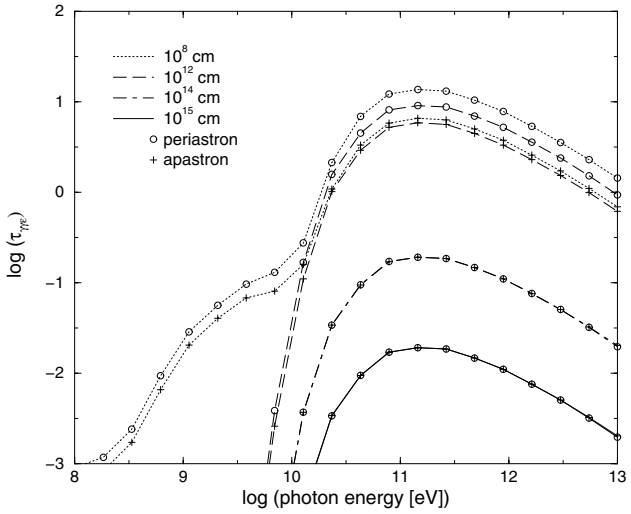

Fig. 2. The photon absorption coefficient as a function of the energy for photons emitted in the jet at different distances from the compact object, at periastron and apastron passages.

extracted from the accretion disk, has been developed in a previous work (Bosch-Ramon et al. 2006). The cold proton plasma and its attached magnetic field, that is frozen to matter and below equipartition, provides a framework where internal shocks accelerate a fraction of the leptons up to very high energies. These accelerated leptons radiate by synchrotron, relativistic Bremsstrahlung with the stellar wind (external) and within the jet (internal), and IC processes. In this model, the external seed photons that interact with the leptons of the jet by IC scattering come from the star, the disk and the corona. A blackbody spectrum is assumed for the star and the disk, and a power-law plus an exponential cut-off spectrum for the corona. The SSC radiation has also been computed as well as the Bremsstrahlung and Compton self-Compton radiation, being the radiation of the last two mechanisms negligible.

The dissipated shock kinetic energy that goes to relativistic particles comes from the mean bulk motion kinetic energy, directly related to the kinetic energy carried by shocks in the plasma. The number of relativistic particles that can be produced along the jet is constrained by the limited capability of transferring energy from the shock itself to the particles, and by the fact that the relativistic pressure must be kept below the cold proton pressure. The particle maximum energy is limited by the acceleration efficiency and the local energy losses in the available space. The acceleration efficiency depends on shock properties: shock strength, shock velocity, magnetic field direction, and diffusion coefficient (e.g., see Protheroe 1999). It has been parametrized due to the lack of knowledge of the specific details of the shock physics for this case.

In our scenario, the jet formation is mainly constrained by a characteristic launching radius, where the ejected matter gets extra kinetic energy from the accretion reservoir, and by the accretion energy reservoir itself, which varies along the orbit. The modeling of the accretion rate changes allows us to introduce variability in a consistent way. Moreover, since the interaction angle between jet leptons and star photons changes with the orbital phase, variability naturally appears at very high energies (see below). Finally, we have approximately computed the effects produced on the SED by the photon absorption under the external photon fields as well as the IC radiation of the first generation of secondaries inside the binary system. In Fig. 2, we show the photon absorption coefficient as a function of the photon energy, at different distances from the compact object, during periastron and apastron passages. It is seen that the corona and disk photon fields (regions of $\sim 10^8$ cm) attenuate slightly the high-energy γ-ray photons in the inner part of the jet. At VHE, star photon absorption dominates for distances $\lesssim 10^{13}$ cm, i.e., within the binary system. At greater distances, absorption goes down to negligible values. Photon absorption is higher at periastron than at apastron passage, due to the dependence of the stellar photon density with the orbital distance, although for large distances from the compact object, the opacities at both orbital phases become equal. Our results are similar to those obtained by Böttcher & Dermer (2005) and Dubus (2006), that present a detailed analysis of the effect of $\gamma\gamma$ absorption of VHE γ-rays near the base of the jet of LS 5039. Moreover, the energy dependence of the opacity on the ambient photon fields to the γ-ray propagation and its variation with the distance is not much different from that obtained for the microquasar LS I +61 303 at its periastron passage (Romero et al. 2005).

Finally, we note that our model does not take into account the radiative contribution from relativistic protons that could be accelerated along with the leptons. These protons can cool through interactions with ions from the stellar wind producing additional γ-ray emission at high energies (Romero et al. 2003, 2005).

3.3. Parameters of the model

The model involves a large number of parameters because it aims at reproducing the broad-band spectrum by taking into account several physical mechanisms. However, in the case of

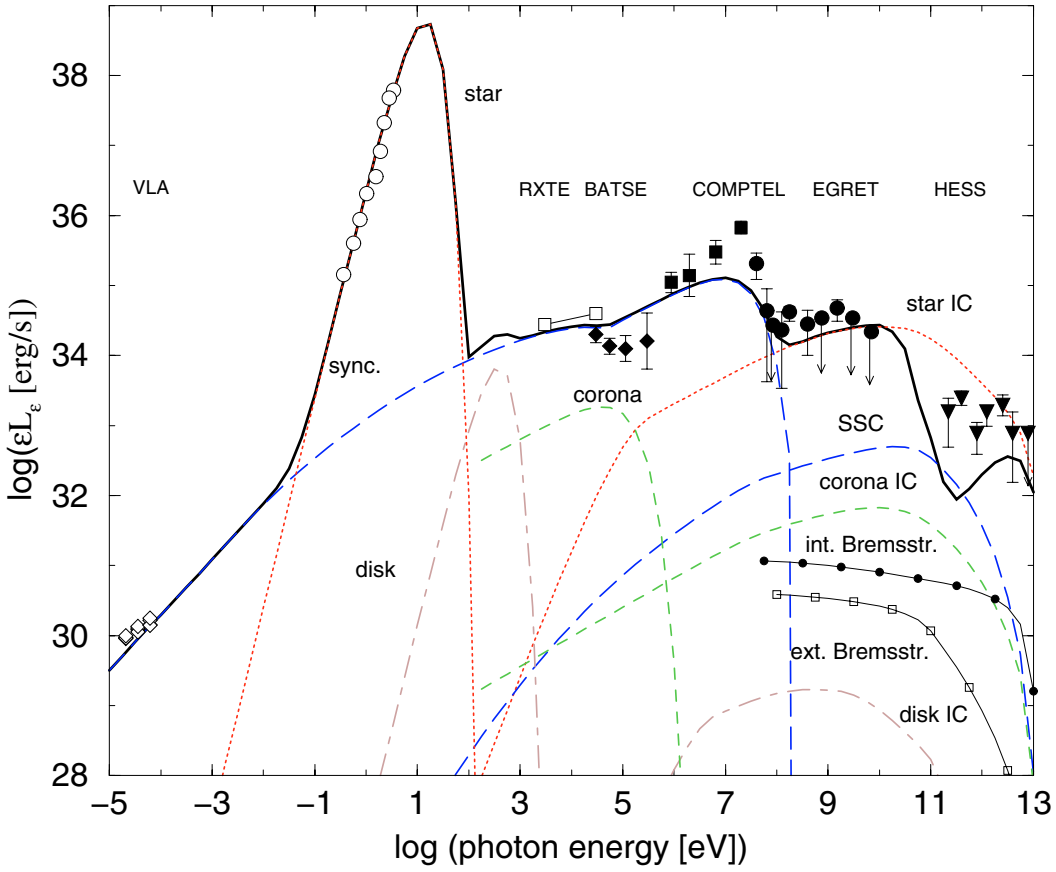

Fig. 3. Comparison of the spectral energy distribution of LS 5039 computed from the present model, at the periastron passage and using the parameters of Table 1, with the observed data. We show the different components of the emission as well as the sum of all of the them, which is attenuated due to $\gamma\gamma$ absorption (solid line). The points observed are from Martí et al. (1998) (VLA, diamond), Clark et al. (2001) and Drilling (1991) (optical, circle, corrected of absorption), Bosch-Ramon et al. (2005a) (RXTE, square), Harmon et al. (2004) (BATSE, diamond filled), Collmar et al. (2003) (COMPTEL, square filled), Hartman et al. (1999) (EGRET, circle filled) and Aharonian et al. (2005a) (HESS, triangle down filled). The arrows in the EGRET and HESS data represent upper limits (3σ).

LS 5039 an important fraction of the parameters are well established from observational data or can be easily estimated from some reasonable assumptions. We call these parameters "primary parameters". The remaining "secondary" parameters can be reduced to a manageable number. In Table 1 we present the primary parameter values of our model. The first half of them are the parameters describing the binary system and their components. We adopt updated values taken from Casares et al. (2005). The electron power-law index (inferred from X-ray photon indices found by Bosch-Ramon et al. 2005a), the jet ejection Lorentz factor (Paredes et al. 2002) and the tangent of the jet semi-opening angle (Paredes et al. 2002) are parameters estimated and/or adopted previously by other authors. Regarding the jet ejection Lorentz factor, although it seems well established that the jet is mildly relativistic (Paredes et al. 2002), no direct jet velocity estimate has been obtained until now and we have fixed the Lorentz factor to 1.1. The values adopted for the disk inner part temperature and the corona photon index correspond to typical values found in other microquasars, because the X-ray spectrum of LS 5039 only provides clear upper limits to the luminosities of both disk ($L_{\rm disk} \simeq 10^{34}$ erg s^{-1}) and corona ($L_{\rm cor} \simeq 10^{34}$ erg s^{-1}) (Bosch-Ramon et al. 2005a). The jet-accretion rate parameter, κ, that gives the ratio between the jet matter injection rate and the accretion rate, has been taken to be similar to observational and theoretical estimates (see, e.g., Fender 2001; Hujeirat 2004).

Next, we describe the secondary parameters of the model, which have been adopted in order to better reproduce different spectral and variability properties of the source. They are summarized in Table 2. The shock energy dissipation efficiency, ξ, that gives the energy dissipated by shocks in the jet, has been taken (Bosch-Ramon et al. 2006) to be at most the quarter of the kinetic energy of the shock to get enough luminosity at energies beyond X-rays[1]. The ratio of the magnetic field (B) energy density to the cold matter energy density has been fixed to $f_B = 0.01$ taking into account X-ray flux constraints from observations (Bosch-Ramon et al. 2005a). The acceleration efficiency parameter, η ($\times q_{\rm e}Bc$), has been fixed such that the maximum energy photons reach the energies at which the source

[1] This does not mean that a quarter of the shock kinetic energy is dissipated through shocks, but that it might be so in case that the energy losses would require it, i.e., the shock could be radiatively efficient up to a 50% of the kinetic energy in the regions where energy losses are very strong (the total jet energy lost through radiation is about 15%).

Table 1. Primary parameter values.

Parameter and unit	Value
e: eccentricity	0.35^a
a: orbital semi-major axis [cm]	2.2×10^{12a}
θ: jet viewing angle [°]	24.9^a
$\dot{m}_{\rm w}$: stellar mass loss rate [$M_\odot$ yr^{-1}]	$\sim 7 \times 10^{-7a}$
$M_{\rm x}$: compact object mass [$M_\odot$]	3.7^a
$R_\star$: stellar radius [$R_\odot$]	9.3^a
$M_\star$: stellar mass [$M_\odot$]	22.9^a
$L_\star$: stellar bolometric luminosity [erg s^{-1}]	7×10^{38a}
$T_\star$: stellar surface temperature [K]	3.9×10^{4a}
p: electron power-law index	2.2^b
$\Gamma_{\rm jet}$: jet injection Lorentz factor	1.1^c
χ: jet semi-opening angle tangent	0.1^c
$kT_{\rm disk}$: disk inner part temperature [keV]	0.1
$p_{\rm cor}$: corona photon index	1.6
z_0: Jet initial point [$R_{\rm Sch}$]	50
κ: jet-accretion rate parameter	0.1^d

[a] Casares et al. (2005); [b] Bosch-Ramon et al. (2005a); [c] Paredes et al. (2002); [d] Fender (2001); Hujeirat (2004).

Table 2. Secondary parameter values.

Parameter and unit	Value
ξ: shock energy dissipation efficiency	0.25
f_B: B to cold matter energy density ratio	0.01
η: acceleration efficiency	0.1
$V_{\rm w}$: equatorial wind velocity [cm s^{-1}]	6×10^7
$\dot{m}_{\rm jet}$: jet injection rate [$M_\odot$ yr^{-1}]	4×10^{-10}
ζ: max. ratio hot to cold leptons	0.1
$r_{\rm l}$: launching radius [$R_{\rm Sch}$]	9
$V_{\rm stream}$: periastron stream velocity [cm s^{-1}]	5×10^6

has been detected by HESS. This value for η is in agreement with that of a strong and transrelativistic shock with a magnetic field parallel to its direction of motion and a diffusion coefficient close to the Bohm limit (Protheroe 1999). The stellar wind velocity in the vicinity of the compact object ($V_{\rm w}$), estimated in Sect. 2, is likely affected by peculiarities of the star (e.g., close to but not suffering Roche-lobe overflow, fast rotation, etc.; see Casares et al. 2005). This velocity implies, along with the known stellar mass loss rate (see Table 1) and assuming isotropic flux, a mean accretion rate along the orbit of $\dot{m}_{\rm acc} \sim 4 \times 10^{-9}\ M_\odot$ yr^{-1} (i.e. ∼5% of the Eddington rate). From this value and κ, the jet matter injection rate can be derived: $\dot{m}_{\rm jet} \sim 4 \times 10^{-10}\ M_\odot$ yr^{-1}. In order to try to satisfy both, the assumption that the jet is cold matter dominated and the observed optically thin nature of the radio spectrum, we have fixed the maximum number of relativistic leptons[2] to be $\zeta = 0.1$ of the total number of particles in the jet. This is higher than the value used by Bosch-Ramon et al. (2006). The implications of this are discussed in Sect. 4. Finally, the launching radius can be estimated to be $\sim 9 R_{\rm Sch}$, since the energy to eject the jet is assumed to be accretion energy transferred and the Lorentz factor is roughly known (Bosch-Ramon et al. 2006).

We note that we are not fitting data but reproducing a broad-band spectrum as a whole. This implies that the values of the parameters used by the model are approximated. The parameters in Tables 1 and 2 not obtained directly from observations have a range of validity within 10% for p, $\Gamma_{\rm jet}$, $kT_{\rm disk}$, $p_{\rm cor}$, $V_{\rm w}$ and $V_{\rm stream}$; and within a factor of a few for z_0, κ, ξ, f_B, η, $\dot{m}_{\rm jet}$, ζ and $r_{\rm l}$.

4. Results

4.1. Spectral energy distribution of LS 5039

Figure 3 shows the computed SED (continuous thick line) of LS 5039 at the periastron passage (phase 0.0) using the physical parameters listed in Tables 1 and 2. We have plotted also the contributions from the star, disk, corona and synchrotron radiation as well as the inverse Compton emission and relativistic Bremsstrahlung. In the same figure we plot also the observational data.

There is a general agreement between the model and the observed data, although there are some discrepancies that require some explanation. First at all, we note that the multiwavelength data were not taken simultaneously, and this can be an important source of discrepancy for any time-dependent model.

At the radio band, the computed spectrum has a spectral index of 0.3, instead of the observed ∼0.5 (Martí et al. 1998, where $F_\nu \propto \nu^{-0.5}$). It seems that an additional process, not contemplated in our scenario, rises up the number of electrons emitting optically thin radio emission (e.g., interactions with the wind or the environment). Concerning the spatial distribution of radio emission along the jet, our computed fluxes at 5 GHz are about 10, 6 and 0.1 mJy for the inner part of the jet (<1 AU), at middle distances from the origin (1–1000 AU) and beyond (>1000 AU), respectively. This roughly reproduces the extended emission of the radio source observed using VLBI techniques (Paredes et al. 2002).

At the X-ray band, most of the emission is synchrotron radiation coming from the relativistic electrons of the jet and only a marginal contribution comes from the disk and almost a null contribution from the corona components (see also, e.g., Markoff et al. 2001). Although the XMM-Newton data does not show evidences of a thermal disk component (Martocchia et al. 2005), we have adopted in our model a disk with moderate luminosity. The role played in the model by this component is negligible, and its contribution appears in Fig. 3 as a small bump over the power-law spectrum below 1 keV. The computed X-ray luminosities and photon indices are very close to those detected so far (see next section and also Bosch-Ramon et al. 2005a).

Gallo et al. (2003) have proposed that radio emitting X-ray binaries, when in the low-hard state, follow a particular correlation concerning radio and X-ray luminosities. In the context of this correlation, LS 5039 is pretty under-luminous at X-rays, presenting a permanent low-hard-like X-ray state. This could be explained by the fact that its radio emission is optically thin, coming mainly from regions outside the binary system,

[2] The number of relativistic leptons is fixed by ξ, ζ, and the condition that their relativistic pressure cannot dominate the cold particle pressure.

instead of being optically thick and completely core dominated (as in the case of models such as the one presented by Markoff et al. 2001; see also Heinz & Sunyaev 2003). As noted above, it might be qualitatively explained by the increase in relativistic electrons predicted by our model, although the issue requires further investigation since our radio spectrum is still too hard.

At BATSE and COMPTEL energies, the main contribution still comes from synchrotron emission of the jet. There is a small disagreement between the predicted luminosity and the one observed by BATSE. However, we note that these data are averaged along many days (Harmon et al. 2004), whereas the plotted SED is computed at phase 0.0, when the accretion is significant though not the highest. At the COMPTEL energy range, as noted above, the moderate disagreement between the computed and observed data is likely produced by the fact that the MeV radiation coming from the COMPTEL source GRO J1823−12, to which LS 5039 is associated, might be a superposition of the MeV emissions of the three different EGRET sources that are in the field of view (Collmar et al. 2003). This means that the data from COMPTEL should be actually taken as an upper limit. In such a case, our computed values would be consistent with the data.

At high-energy γ-rays (0.1–10 GeV), the computed luminosities are similar to those observed by EGRET while the computed photon indices are slightly harder. This fact could be naturally associated with the low temporal resolution of EGRET, with the shortest viewing periods spanning for one week and providing time averaged spectra that could mask harder ones. We note however that, because of the possible effect of pair creation in the jet, the slopes of the SEDs at high-energy γ-rays, unlike the computed luminosities, are not very reliable (see Bosch-Ramon et al. 2006). The dominant component at this band of the spectrum is star IC, whereas the synchrotron radiation is only important at the lower part of EGRET energies. The emission of secondary pairs created within the binary system is not significant.

At VHE γ-rays, star IC emission dominates. The spectrum reaches several TeV, and it is limited by the maximum particle energy, which can reach ∼10 TeV. The contribution of the star IC scattering is favored during the periastron passage due to a higher photon density as well as a smaller interaction angle between the electrons and the photons, which influences the IC scattering. The contribution from the SSC component is minor, although it is more significant at apastron than at periastron. The VHE spectrum is strongly affected by the $\gamma\gamma$ opacity due to pair creation within the binary system, the absorption being stronger at the periastron passage. Therefore, an important decrease of the emission as well as an additional source of variability at those energies appear unavoidable. Also, a hardening of the emission, as seen in Fig. 3, could take place. Our model underestimates the TeV emission, although the difference is less than one order of magnitude. Possibly, some high energy processes involving particle acceleration and emission are taking place in the jet at middle scales, where the 100 GeV photon absorption is not important. This could also be related to the optically thin nature of the radio emission. This outer emission would not be as variable as the emission from the compact jet. In any case, a deeper treatment at this energy band concerning VHE emission and pair creation phenomena is required (Khangulyan & Aharonian 2006).

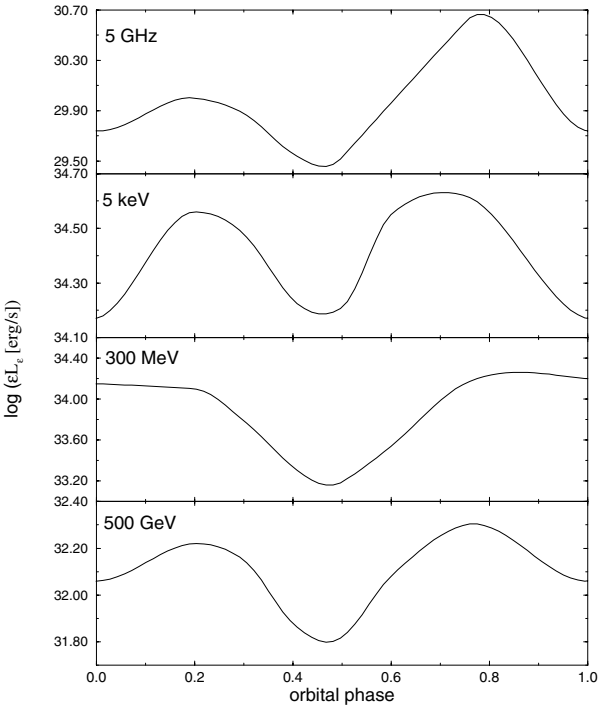

Fig. 4. The panel shows the flux variations along the orbit for the four energy bands considered here. We note that emission at very high-energy γ-rays is strongly attenuated by the photon absorption in the star photon field.

The results obtained by applying other leptonic models (e.g. Bosch-Ramon et al. 2005b; Dermer & Böttcher 2006) do not differ substantially from the comprehensive model presented here, which can explain the broad-band emission from LS 5039. Otherwise, hadronic models can reproduce the emission at VHE energies (Romero et al. 2003) though it is hard to explain how typical EGRET fluxes could be achieved (Romero et al. 2005). Comparing both types of model, it seems that the leptonic ones can explain better than the hadronic ones the broadband spectrum at least up to ∼1 GeV. Both are suitable at higher energies since the energetic requirements are not as strong as those to explain the whole emission from the source.

4.2. Variability properties of LS 5039

Once the accretion model has been applied to reproduce roughly the X-ray lightcurve, we explore what are the consequences at the other bands of the spectrum. In Fig. 4 we show the flux variations along the orbit at four energy bands. At radio and X-ray energies, the predicted flux variations are well correlated with accretion, since they have similar shapes to the accretion orbital curve (see Fig. 1). The predicted amplitude variations are of about one order of magnitude in radio and a factor of three at X-rays, although we note that, if the radio emitting region is large enough, say 10^{15} cm, the variations at these wavelengths will be significantly smoothened by light crossing time limitations (as it seems to be the case, see Ribó (2002).

The variations of the radio spectral indices along the orbit are not treated here, due to the model limitations at radio. However, we mention that the X-ray photon index shows a trend similar to that found by Bosch-Ramon et al. (2005a), i.e. higher fluxes when harder spectra. Nevertheless, the anticorrelation is not as strong as that observed. Emission at EGRET energies varies almost one order of magnitude, although the shape of the lightcurve is different because of the higher rate of IC interaction during phase 0.0 due to angular effects. At VHE, however, the emission is strongly absorbed by the stellar field, producing a dip around periastron passage. At phases 0.6–0.9, there is a long standing peak that is related to the stream related peak at phase 0.7 (0.8) that is not close enough to the stellar companion for banishing due to $\gamma\gamma$ absorption. A similar peak seems to be present in HESS data (Aharonian et al. 2005a) when folded in phase with the new ephemeris of Casares et al. (2005), although further observations should be carried out to confirm this. At phases 0.2–0.3, a smaller peak is seen, which might be detected eventually in future VHE observations. We note that, as it is seen in Fig. 2, if TeV emission comes from distances typically larger than the semi-major orbital axis it would not be significantly attenuated by photon absorption. In such a case, variability would be limited by the size of the emitting region.

5. Comments and conclusions

We have applied to the microquasar LS 5039 a cold matter dominated jet model that takes into account accretion variability, the jet magnetic field, particle acceleration, microscopic energy conservation in the jet, and pair creation and absorption due to the external and internal photons, as well as the emission from the first generation of secondaries under the external photon fields.

The computed SED from radio to VHE γ-rays has been compared with the available observational data, gathered at different bands of the electromagnetic spectrum, showing in general a good agreement. Although the model is limited by its phenomenological nature, we can extract some general conclusions that could be useful to understand the physics behind these objects as well as for going deeper in more basic theoretical aspects concerning the jet plasma characteristics, particle acceleration and jet formation phenomena. In particular, in the context of our model, we can state that the jets are radiatively efficient ($\sim$15%) and sites of particle acceleration up to multi-TeV energies. Otherwise, accretion processes are radiatively inefficient.

The strong absorption of VHE γ-rays by the stellar photon field seems to make hard the detection of high fluxes of radiation if they are generated in the inner regions of the jet, closest to the compact object. Possibly, since the source is not very faint at these energies, some high energy processes involving particle acceleration and emission are taking place in the jet at middle scales, where the 100 GeV photon absorption is not important. This could also be related to the high fluxes and optically thin nature of the radio emission. Variability at these energy bands could provide information about the location of the particle acceleration processes and emitting regions.

Changes in the accretion rate due to the orbital eccentricity and a particular wind density profile can explain the spectral and variability properties observed at X-rays. It hints to a companion stellar wind that is not spherically symmetric nor fast in the equator, since otherwise the γ-ray radiation could not be powered.

We conclude that, with reasonable values for the different parameters, our model seems to be good enough as to describe the general features of the spectrum of LS 5039 from radio to TeV γ-ray energies, the leptonic model being a reasonable candidate for explaining the γ-ray emission on energetic grounds.

Acknowledgements. We thank Marc Ribó for fruitful discussions as well as useful comments and suggestions on the subject studied here. J.M.P. and V.B.-R. acknowledge partial support by DGI of the Ministerio de Educación y Ciencia (Spain) under grant AYA-2004-07171-C02-01, as well as additional support from the European Regional Development Fund (ERDF/FEDER). During this work, V.B.-R. has been supported by the DGI of the Ministerio de (Spain) under the fellowship BES-2002-2699. G.E.R. is supported by the Argentine Agencies CONICET (PIP 5375) and ANPCyT (PICT 03-13291).

References

Aharonian, F., Akhperjanian, A. G., Aye, K. M., et al. 2005a, Science, 309, 746
Aharonian, F., Anchodorqui, L. A., Khangulyan, D., & Montaruli, T. 2005b, submitted [arXiv:astro-ph/0508658]
Bosch-Ramon, V., & Paredes, J. M. 2004a, A&A, 417, 1075
Bosch-Ramon, V., & Paredes, J. M. 2004b, A&A, 425, 1069
Bosch-Ramon, V., Paredes, J. M., & Ribó, et al. 2005a, ApJ, 628, 388
Bosch-Ramon, V., Romero, G. E., & Paredes, J. M. 2005b, A&A, 429, 267
Bosch-Ramon, V., Romero, G. E., & Paredes, J. M. 2006, A&A, 447, 263
Böttcher, M., & Dermer, C. D. 2005, ApJ, 634, L81
Casares, J., Ribó, M., Ribas, I., et al. 2005, MNRAS, 364, 899
Clark, J. S., Reig, P., Goodwin, S. P., et al. 2001, A&A, 376, 476
Collmar, W. 2003, Proc. 4th Agile Science Workshop, Frascati, Rome on 11–13 June 2003, 177
Dermer, C. D., & Böttcher, M. 2006, ApJ, in press [arXiv:astro-ph/0512162]
Drilling, J. S. 1991, ApJS, 76, 1033
Dubus, G. 2006, A&A, 451, 9
Fender, R. P. 2001, MNRAS, 322, 31
Gallo, E., Fender, R. P., & Pooley, G. G. 2003, MNRAS, 344, 60
Harmon, B. A., Wilson, C. A., & Fishman, G. J., et al. 2004, ApJS, 154, 585
Hartman, R. C., Bertsch, D. L., & Bloom, S. D., et al. 1999, ApJS, 123, 79
Heinz, S., & Sunyaev, R. A. 2003, MNRAS, 343, L59
Hujeirat, A. 2004, A&A, 416, 423
Kaufman Bernadó, M. M., Romero, G. E., & Mirabel, I. F. 2003, A&A, 410, L1
Khangulyan, D., & Aharonian, F. A. 2006, in preparation
Kniffen, D. A., Alberts, W. C. K., Bertsch, D. L., et al., 1997, ApJ, 486, 126
Leahy, D. A. 2002, A&A, 391, 219
Markoff, S., Falcke, H., & Fender, R. 2001, A&A, 372, L25
Martí, J., Paredes, J. M., & Ribó, M. 1998, A&A, 338, L71
Martocchia, A., Motch, C., & Negueruela, I. 2005, A&A, 430, 245

Massi, M., Ribó, M., Paredes, J. M., et al. 2004, A&A, 414, L1
McSwain, M. V., Gies, D. R., Riddle, R. L., Wang, Z., & Wingert, D. W. 2001, ApJ, 558, L43
McSwain, M. V., Gies, D. R., Huang, W., et al. 2004, ApJ, 600, 927
Mirabel, I. F., & Rodríguez, L. F. 1999, ARA&A, 37, 409
Motch, C., Haberl, F., Dennerl, K., Pakull, M., & Janot-Pacheco, E. 1997, A&A, 323, 853
Paredes, J. M., Martí, J., Ribó, M., & Massi, M. 2000, Science, 288, 2340
Paredes, J. M., Ribó, M., Ros, E., et al. 2002, A&A, 393, L99
Protheroe, R. J. 1999, in Topics in Cosmic-Ray Astrophysics; Horizons in World Physics, 230, ed. M. A. DuVernois (Nova Science Publishers, Inc., Commack, New York), 247
Ribó, M. 2002, Ph.D. Thesis, Universitat de Barcelona
Ribó, M., Paredes, J. M., Romero, G. E., et al. 2002, A&A, 384, 954
Ribó, M., Negueruela, I., Blay, P., Torrejón, J. M., & Reig, P. 2006, A&A, 449, 687
Romero, G. E., Torres, D. F., Kaufman Bernadó, M. M., & Mirabel, I. F. 2003, A&A, 410, L1
Romero, G. E., Grenier, I. A., Kaufman Bernadó, M. M., Mirabel, I. F., & Torres, D. F. 2004, ESA-SP, 552, 703
Romero, G. E., Christiansen, H., & Orellana, M. 2005, ApJ, 632, 1093
Strong, A. W., et al. 2001, AIP Conf. Proc., 587, 21
Zhang, S., Collmar, W., & Schönfelder, V. 2005, Ap&SS, 297, 283